

Satellite observations using the Chilbolton radar during the initial ESA ‘CO-VI’ tracking campaign

J. D. Eastment⁽¹⁾, D. N. Ladd⁽²⁾, C. J. Walden⁽¹⁾ and M. L. Trethewey⁽³⁾

*⁽¹⁾STFC Rutherford Appleton Laboratory,
Chilton, Didcot, Oxfordshire, OX11 0QX, U.K.
Email: jon.eastment@stfc.ac.uk*

*⁽²⁾STFC Chilbolton Observatory,
Drove Road, Chilbolton, Stockbridge, Hampshire, SO20 6BJ, U.K.*

*⁽³⁾Control Loop Concepts Ltd.,
51, South Street, Lewes, East Sussex, BN7 2BU, U.K.*

INTRODUCTION

The Chilbolton radar, a high-power S-band system equipped with a fully-steerable 25 m diameter dish antenna, has hitherto been used almost exclusively for meteorological and atmospheric science-based research. This radar was recently modified for use as a tracking asset in support of ESA’s Space Situational Awareness Preparatory Programme (SSA PP). In late November and early December of 2010, the radar participated in a set of satellite tracking measurements comprising the first campaign of the SSA PP’s ‘CO-VI’ activity.

This initial campaign involved observations of the satellites ENVISAT, METOP-A, CRYOSAT-2, GRACE-1, JASON-2, PROBA-1 and STARLETTE. In addition to these ESA-mandated objects, we also tracked the ISS, AQUA, COSMOS_1346, COSMOS_1782 and many IRIDIUM satellites. In subsequent CO-VI tracking campaigns during April and May 2011, over 40 different satellites were successfully observed resulting in several hundred recorded track-files. These included targets which had mechanically-scanned instruments; which were tumbling; which had interesting polarimetric signatures; and which performed on-orbit manoeuvres.

In this paper, we report the details of the modifications to the Chilbolton radar which were necessary in order to adapt it for SSA work. We present examples of the satellite tracks obtained, and comment on interesting features noted in the data. We compare the calculated sensitivity of the radar in its current configuration with the results obtained in practice. We outline our future plans for upgrading the radar’s hardware and software, so as to improve detection performance against small-RCS targets. Finally, we discuss the use of the upgraded radar for Space Object Identification and characterisation by exploiting both its wideband waveform and polarimetric capabilities.

CHILBOLTON OBSERVATORY SITE

The Chilbolton Observatory is an outstation of the Science and Technology Facilities Council’s (STFC) Rutherford Appleton Laboratory (RAL). RAL’s Chilbolton Group comprises 10 scientists and engineers working in the general areas of radio communications, radiowave propagation, radar remote sensing and atmospheric science research. The staff are split between the RAL Chilton site and the Chilbolton Observatory, near Stockbridge in Hampshire, where the 25 metre dish is located (Fig. 1). The Observatory has a permanent staff of 5, comprising scientists, engineers and specialist electrical and mechanical support technicians for the 25 m dish.

The engineers at Chilbolton are experienced in RF and microwave systems, data acquisition, computer networking and dish operations. The Observatory is connected to the Internet via a high-speed fibre-optic link, which is well-suited for transferring large recorded data-sets from radar measurement campaigns. Additionally, software has been developed to allow control of the dish, radars and associated equipment from a remote terminal, with real-time display of relevant measured parameters.

Dormitory and cooking facilities are available on-site to support dish operations outside of office hours and at weekends. The site has full telephone, fax, e-mail and web connectivity. All these facilities are available to visiting experimenters.

The 25 m dish, which is the main facility at the Chilbolton site, is shown in Fig. 2. The dish is fully steerable in both azimuth and elevation, and is controlled via a PC-based system. An orbital prediction program generates azimuth and elevation antenna pointing data from Two Line Element (TLE) sets obtained from the NORAD Spacetrack web-site. These data are combined with NTP-derived time to facilitate real-time tracking. STFC operates several radars installed on the 25m dish. For the purposes of the CO-VI campaign, all data were recorded using the specially-modified Chilbolton Advanced Meteorological Radar (CAMRa).



Fig. 1. Aerial view of the Chilbolton Observatory site



Fig. 2. The 25 m fully-steerable dish

RADAR SYSTEM

The CAMRa radar is described in [1]. For SSA use, it was modified to achieve the specification detailed in Table 1. In this campaign, no *a priori* knowledge of target range (based on the TLE) was used in the signal processing algorithm. Consequently, a PRF of 71.428 Hz, corresponding to a PRI of 14.0 ms and a maximum unambiguous range of 2100 km, was chosen so as to achieve alias-free range measurements for targets in low-earth orbit (LEO). Under these conditions, although the peak power is some 700 kW, the average transmitted power is only 25 W. The system's polariser was configured to transmit pulses of fixed, horizontal polarisation, while the radar's receivers simultaneously recorded both co-polar (horizontal, H) and cross-polar (vertical, V) target returns. The theoretical single-pulse signal-to-noise ratio (SNR) as a function of target radar cross-section (RCS) and range (as determined from the standard radar equation) is shown in Table 2.

Table 1: Specification of the modified CAMRa radar

Parameter	Value and comments
Operating frequency	3076.5 MHz
Antenna gain	53.5 dBi
Beamwidth	0.28° (FWHM; -3 dB, 1-way)
Polarisation	Tx: H; Rx: H and V
Transmitter type	Cavity magnetron
Peak power	700 kW
Average power	25 W
Pulse repetition frequency	71.428 Hz
Pulse width and coding	0.5 μ s, un-coded rectangular
Receiver type	Superhet, log and I/Q channel
Noise figure	3.5 dB, plus duplexing losses (\sim 2dB)
IF centre freq. and bandwidth	30 MHz centre, 4 MHz BW
Data acquisition system	7 channels, 12-bit / channel

Table 2: Calculated SNR as a function of RCS and range

RCS / m ²	SNR (dB) at range of 500 km	SNR (dB) at range of 1000 km	SNR (dB) at range of 2000 km
0.1	+9	-3	-15
0.2	+12	+0	-12
0.5	+16	+4	-8
1	+19	+7	-5
2	+22	+10	-2
5	+26	+14	+2
10	+29	+17	+5

DISH CONTROL AND TRACKING SYSTEM

The 25 m antenna system is versatile and can support operations in areas as diverse as weather radar, radio astronomy, satellite in-orbit testing (IOT), and space surveillance and tracking. It can achieve this because of the adaptable way in which the hardware and software have been designed and implemented.

Antenna Drive System

The antenna uses an Az / El mount, and can slew up to 1 deg / sec in elevation and up to 3 deg / sec in azimuth. A new drive system, installed in 2008, uses 6 vector drive AC motors: four in azimuth, and two in elevation. Speed and torque control of the motors is achieved by sophisticated servo drive amplifiers. Elevation backlash is minimised by an over-balance condition of the antenna, which ensure the gears are always meshed on one face. The azimuth backlash is minimised by implementation of a torque bias with one motor. Position reference relies on absolute encoders, which can resolve the antenna position to $1/480^{\text{th}}$ (0.002083) of a degree. Position accuracy has been checked by tracking radio-stars such as Cassiopeia A, while peaking the signal in the receiver by introducing azimuth and elevation offsets.

Fast Feed Changer

The 25 m antenna feed system employs a feed changer (a remotely-controlled, motorized, 3-axis linear positioner) to allow feed assemblies for different operational activities to be moved into the prime-focus. The Fast Feed Changer (FFC) can accommodate up to four feeds. Movement of the FFC in X and Y (in the plane of the focus) changes the feed. Movement in Z allows one feed to be moved to the focal plane, while the others are moved back to improve inter-feed isolation. Incremental movements in X, Y, and Z can be conducted to optimise the gain and symmetry of the beam. Control of the FFC is via ASCII commands conveyed on a serial interface. A feed change can be conducted remotely in a matter of minutes.

Polarisation Switch

The radar feed assembly has a mechanical polarisation switch, which is based on waveguide windows in a rotating disk which alternately allow H and V pulses to be transmitted. The alignment of the window in the disk with the waveguide is detected by an electro-optical sensor which generates a pulse that is used to trigger the transmitter. The motor drive speed can be controlled remotely to change the PRF. The motor can also be commanded to move the disk to a specific location, corresponding to H or V, and to hold it in place. In this mode, the trigger pulses must be generated externally – as is the case when the radar is used in SSA mode, when a crystal-controlled pulse-generator determines the PRF.

Satellite Tracking Modes

The antenna has different slewing modes dependent on the tracking requirements. Command of the antenna is by an ASCII-coded serial interface. There are different high-level programs which can be executed on the Linux OS Command Computer to allow the operator to task the antenna in the appropriate mode. The high gain of the antenna results in a narrow beam which requires the antenna tracking to be accurate in order to keep a satellite in the beam. The antenna does not currently utilise a monopulse feed system, hence it cannot use receiver error signals to lock onto a target. The antenna tracking has to rely on predicted target orbits in order to calculate the necessary look-angles.

There are two modes for tracking satellites, namely position nudges and velocity slewing:

The position nudge mode is suitable for slow-moving targets, such as MEO and GEO satellites, and for celestial objects such as the sun, moon and stars. In this mode, the antenna is requested to move in incremental nudges between the setpoints which are the demand positions for an instant in time. Each nudge is a sequence of acceleration, constant velocity, and deceleration periods which are calculated by a trajectory generator. The setpoints are made available in a formatted file, or are acquired in real-time from a position server running on a local computer by means of a TCP/IP interface. The effective maximum slewing velocity of the antenna when tracking these objects is 0.2 deg / sec. The timing reference for the track comes from the command computer, which is synchronised to UTC using Network Time Protocol (NTP).

The velocity slewing mode is essential for tracking faster-moving targets, such as LEO satellites. The drives are fed a velocity profile which the antenna needs to follow in order to track the satellite. The velocity profile is derived in

advance using a polynomial-based formula to calculate the first derivative of the positions which are read from a high resolution position setpoint data file. The setpoint data file is generated using a program that computes the track based on orbit prediction. The antenna controller feeds the velocity demands to the motor servo drive amplifiers after the addition of a position feedback term which reflects the current position error. The antenna controller does not keep accurate absolute time; hence, the absolute timing is referenced from the command computer - which maintains accurate time through NTP.

There is an inherent latency in the time taken for the command message containing the velocity and position information to be applied to the drive. Left unaccounted for, this lag could result in significant position tracking errors. The error due to this lag is minimised by looking ahead in the data file by a constant time increment, so that the data is applied at the drive at the correct instant. This advance time increment was determined by plotting, for different time shifts, the error between the demand position and the recorded position, against demand position. The curve yielding the smallest RMS difference was the one with a time shift of 0.21 seconds. The effect of this time advance was checked by observing the tracking error for a variety of different satellite tracks, and confirmed by successfully detecting the designated spacecraft in the radar beam.

The look-angles required to track specific satellites are computed from TLEs using SDP4 / SGP4 code running in a program called 'predict'. This is an open-source program that is compiled to run under the Linux OS. The version of 'predict' running on the command computer has been modified to output higher-resolution position data. 'predict' operates a server-mode, from which the data are provided via a TCP/IP interface to the tracking program. Alternatively, it can be run in a command-line mode to prepare the position setpoint files in advance. The velocity setpoint files are prepared by feeding the position setpoint data into a program called 'chobs_trk', which unwinds and shifts the positions into the correct range for the 25 m antenna, then derives the velocities using a polynomial smoothing technique.

It is important to use TLEs which are as current as possible. A script, scheduled to run in the morning prior to the start of tracking operations, downloads the full Space Track catalogue of TLEs onto the command computer. Another script then selects the desired TLEs for the objects which are to be tracked, and creates a 'tle' file for 'predict'. Updates to the TLEs, and to the list of objects to be tracked, can be conducted at any time. A daily archive of tracking operations is automatically generated, and is kept for future reference.

Satellite Tracking Procedure

The following procedure is executed by the radar operator in order to conduct an upcoming satellite pass. Prior to the AOS time of the target satellite, the track file must be generated using the 'predict' and 'chobs_trk' commands. Display output from the 'chobs_trk' program includes the track start time and position. The antenna is commanded to slew to the specific azimuth and elevation position, allowing sufficient time to reach the starting point. The antenna will automatically begin to move when the start time of the track is reached. The start elevation is typically set to -1.0 degrees to ensure that the antenna has settled accurately on-track when the satellite comes above the horizon. Once the antenna has reached a suitable elevation (typically a few degrees, so as to avoid atmospheric refractive effects), and the satellite is within range, the data acquisition system starts recording.

DATA ACQUISITION AND RECORDING

In designing the setup for this experiment, a PRF of 71.428 Hz was selected (ie: a pulse repetition time of 14.0 ms) to allow a maximum unambiguous range of 2100 km. Unfortunately, there appeared to be problems triggering the current data acquisition (DAQ) card at this PRF, which had not been present at the higher PRF usually employed for the meteorological applications of this radar. To overcome this, a scheme was devised to allow the DAQ card to be triggered four times for each transmitted pulse. This scheme does introduce a further complication, however. It is not guaranteed that the data recorded following the first of the four DAQ triggers will be closest in time to the outgoing transmitted pulse (i.e. correspond to the nearest range gates). Fortunately, by examining the data recorded in the 19th range-gate, the correct DAQ synchronisation may be identified by the presence of a saturated signal in the co-polar channel. In practice, it was found that correct synchronisation came from selecting either the first or third DAQ trigger. For the experiments described here, the recorded data represent an average over four pulses. Hence, to allow for the above triggering and synchronization scheme, the system was configured to trigger data acquisition 18 times per ray.

The data were stored in NetCDF format, using an adaptation of the scheme normally employed for the meteorological use of this radar. For each DAQ trigger, data were recorded at a sequence of 75 m range gates. The number of gate

samples recorded was selected so that data from the last of each set of four DAQ triggers remained unambiguous and did not incorporate the next transmit pulse. A side-effect of this configuration is that it introduces intermediate “blind” range intervals. Hence, apart from an overall range calibration offset, the data correspond to the four intervals, namely $([0.075, 517.575] + n \cdot 525)$ km, with $n = 0, 1, 2, 3$. In other words, the first blind range interval is from 517.575 to 525.075 km, with the second and third such intervals offset from this by 525 and 1050 km, respectively. The range stored in the NetCDF files refers to the $n = 0$ interval, and the values denote the (uncalibrated) centres of each gate. There is a further blind range interval around zero-range due to saturation from the transmit pulse, but this does not pose any problems for the satellite targets of interest here. The co-polar received signals are stored as ZED0, ZED1, ZED2 and ZED3, with ZED0 being identified $n = 0$, etc. Similarly, ZED_X0, ZED_X1, and so on, denote the cross-polar returns. No range-dependent correction has been applied to the signal strengths.

Each NetCDF file was post-processed to provide a CCSDS-format TDM (tracking data message) file. The results described here have been derived via a simple scheme in which the target range was identified with the range gate corresponding to the strongest co-polar signal (excluding the lowest saturated gates).

The value of the co-polar signal strength for the selected gate is included in the TDM file. A limitation of this algorithm is that whenever the target signal momentarily falls, the selected strongest signal will typically correspond to noise in some arbitrary range gate. Further refinement of the algorithm is needed to identify and to remove these spurious values.

The range was calibrated by comparison with a readily identifiable terrestrial target (a transmitter mast). The gate containing the maximum co-polar signal (ZED0) was located, and the range offset derived from the difference between the radar-measured range of the gate centre and the known target range (calculated from Ordnance Survey map references for the radar and the mast using simple trigonometry). The value of the offset was found to be -1.48 km.

QUICK-LOOK PLOTS

Quick-look plots were produced from the TDM files. Two examples, for the GEO-IK-2 and ADEOS satellites, which will be referred to later, are shown in Figs. 3 and 4.

In each case, the top panel shows the target range identified by the above algorithm. There is one colour-coded dot for each time-stamp in the TDM file, the colours being an indication of co-polar signal strength (in dB). For clarity of presentation, the plotting sequence has been ordered to ensure that strongest signals are plotted in front of weaker ones. The black line corresponds to the predicted target range as derived from the TLE.

The second panel provides a time-series plot of the co-polar signal strength (in blue) as identified by the above algorithm. The red trace is the cross-polar signal for the same range gates.

The lower two panels show the time-variation of the antenna azimuth and elevation.

RESULTS FROM THE INITIAL CO-VI CAMPAIGN

Fig. 5 (a-d) shows typical quick-look plots of the tracks from METOP-A, ENVISAT, CRYOSAT-2 and GRACE-1. These objects were consistently detected on most passes. JASON-2 was marginally detected on several passes, but the SNR was not sufficient to form a track. The objects PROBA-1 and STARLETTE, which had the lowest RCS, were not detected. It was noted that, in general, the radar returns are very variable throughout a pass – much more so than would be expected due to the simple $1/r^4$ dependence of SNR on range for a point-target. This is presumably due to a complex dependence of the objects’ RCS as a function of sensor viewing angle. Some targets, eg: GRACE-1, exhibit a specular-reflection ‘glint’ at the closest point of approach (CPA). We assume that this is due to the nadir-pointing flat underside panel of the satellite bus.

OBSERVATIONS OF OTHER SATELLITES

In total, over 40 different satellites have been observed during the CO-VI tracking campaigns in November / December 2010, in April 2011, and in May 2011. Examples of the tracks obtained from some of the additional objects observed during the November / December 2010 campaign are shown in Fig. 6 (a-d). In addition, some interesting objects were observed which had unusual radar target phenomenologies. These are briefly described below.

Detection of a Mechanically-Scanned Instrument

When observing AQUA, it had been noticed that the radar's A-scope display exhibited a consistent amplitude fluctuation with a well-defined period. A segment of time-series data from the radar's logarithmic detector channel was transformed into the frequency domain using a Matlab routine. The resultant spectrogram, shown in Fig. 7 (a), clearly reveals a set of spectral lines at 0.66 Hz (39.5 r.p.m.), and at multiples thereof. The NASA web-site for AQUA [2] indicates that the satellite's AMSR-E instrument employs a 1.6 m diameter antenna, which is continuously rotated at 40 r.p.m. The signature of this scanning antenna dominates this large satellite's overall RCS, and is clearly responsible for the fundamental frequency component seen in the measured spectrogram. The signals at multiples of 0.66 Hz are thought to be due to specular-reflection glints from the antenna's reflector support struts.

Detection of a Tumbling Object

Reports within the aerospace community [3] indicated that the recently-launched geodesy satellite, GEO-IK-2, had been injected into an incorrect orbit. Furthermore, it was suspected that the satellite may not have been under positive attitude control. Chilbolton observations resulted in the quick-look plot shown in Fig. 3. The second panel of Fig. 3 shows strong evidence of periodic signal fluctuations in the time-series plots of co- and cross-polar returns. A spectrogram derived from this time-series, shown in Fig. 7 (b), indicates a clear peak at 0.47 Hz (28.2 r.p.m.). However, there is a slightly weaker spectral line at half this frequency, suggesting that the fundamental rotational rate is actually 14.1 r.p.m. We therefore conclude that the satellite was indeed tumbling at the time of our radar observation, and that the rate of tumbling was 14.1 r.p.m. (or possibly a sub-multiple of this figure, depending on which structural element(s) of the satellite are the dominant scatterer(s)).

Cross-Polarisation Effects

Simultaneous A-scope observations of the fluctuation of the co-polar and cross-polar returns from several satellites have shown that there are times when the SNR in the cross-polar channel can greatly exceed that in the co-polar channel. An example of this phenomenon is shown in Fig. 8 (a-b) for the ADEOS satellite. The 75 m-resolution tracks in Fig. 8 (a-b) represent a segment of the full pass, shown in the quick-look plot of Fig. 4. This is a signature of multiple reflections from structural elements on the satellite (eg: flat panels of the bus, solar panels, booms, antennas, etc.). A single reflection could not produce a cross-polar signal which exceeds the level of the co-polar return. Therefore, the variation in the ratio of cross-polar to co-polar signal level throughout a pass contains information on the structural geometry of the target satellite.

FUTURE WORK

In the immediate future, Chilbolton plans to participate in the CO-VI beam-park experiment. In the longer term, we hope to contribute to the tracking campaigns planned for the next phase of the ESA SSA PP, under core activity CO-VIII. A new transmitter (TMD Ltd., model PTX-7610) has recently been purchased. This unit will provide up to 1.3 kW average power (60 kW peak), with a bandwidth capability of 2.7 to 3.1 GHz. In addition, an AR-320 transmitter, part of a UK Type-93 radar system, has been secured for SSA use at Chilbolton. This equipment can produce a maximum average power of 4 kW (150 kW peak) over the band 3.1 to 3.5 GHz, representing an increase in sensitivity of some 22 dB over the existing system – greatly increasing the radar's capability to detect low-RCS targets. Either of these transmitters, combined with a new receiver and data acquisition system, and exploiting coherent signal processing techniques, will open-up many new possibilities for future SSA work. In particular, we plan to exploit the upgraded radar's Doppler, polarimetric and wide-bandwidth capabilities to measure target velocity and acceleration, as well as object shape, structural characteristics, and dynamics. In the longer term, it is planned to work towards a high-range resolution (HRR) profiling and inverse synthetic aperture radar (ISAR)-based target imaging capability.

REFERENCES

- [1] J. W. F. Goddard, J. D. Eastment and M. Thurai, 'The Chilbolton Advanced Meteorological Radar: a tool for multidisciplinary atmospheric research'. IEE Electronics and Communications Engineering Journal, **6**(2), 77-86. 1994.
- [2] NASA AQUA web-site: http://aqua.nasa.gov/about/instrument_amsr.php Accessed on 24 th May, 2011.
- [3] RussianSpaceWeb.com: http://www.russianspaceweb.com/geo_ik2.html Accessed on 24 th May, 2011.

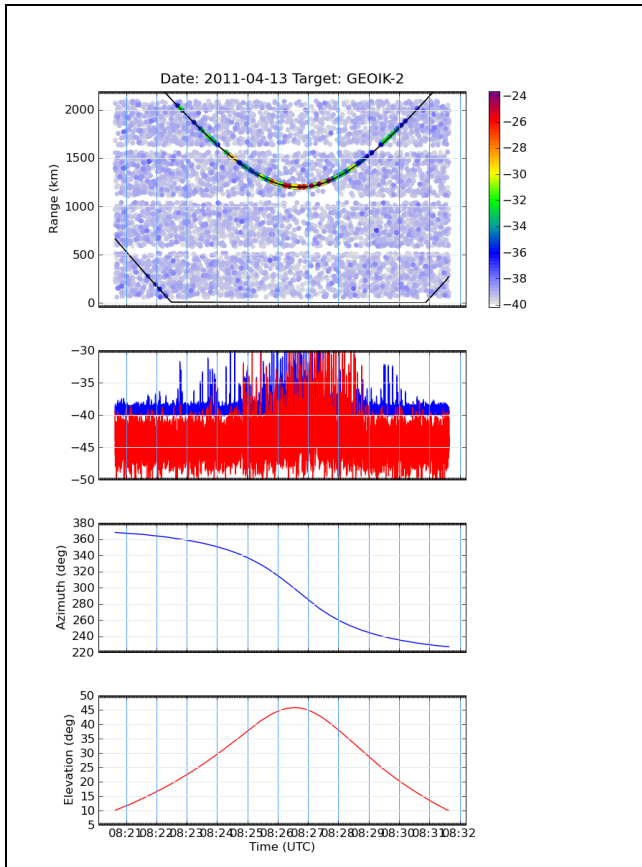


Fig. 3. Quick-look plot for GEO-IK-2 satellite pass

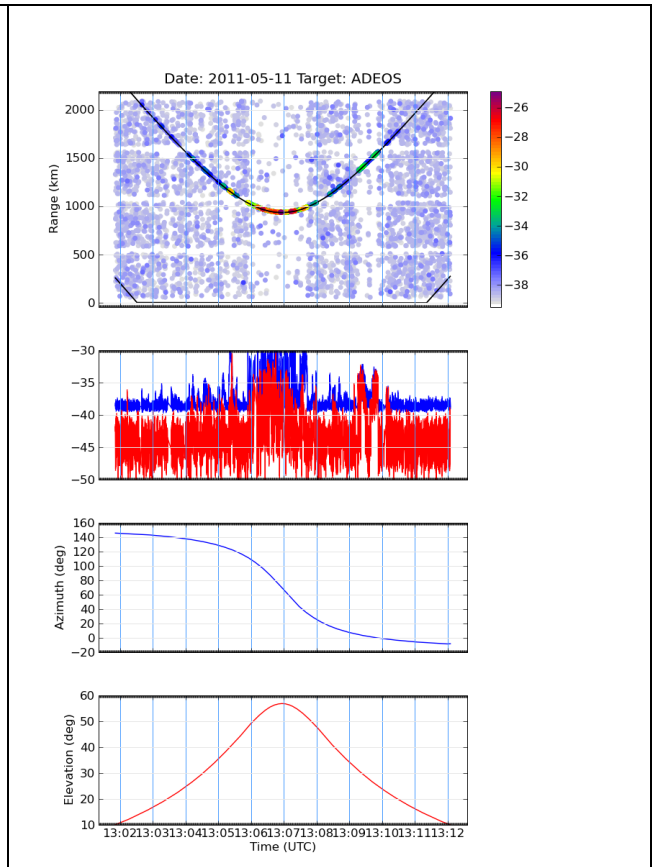


Fig. 4. Quick-look plot for ADEOS satellite pass

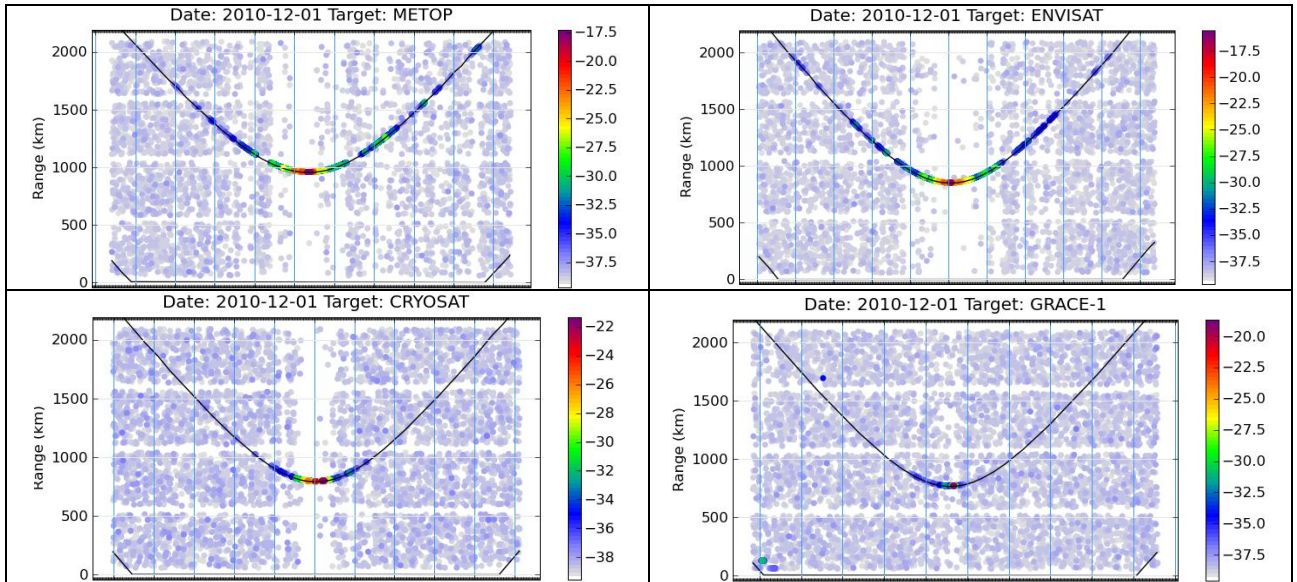


Fig. 5 (a-d). Tracks for a) METOP-A, b) ENVISAT, c) CRYOSAT-2 and d) GRACE-1: the designated objects for the initial ESA 'CO-VI' tracking campaign

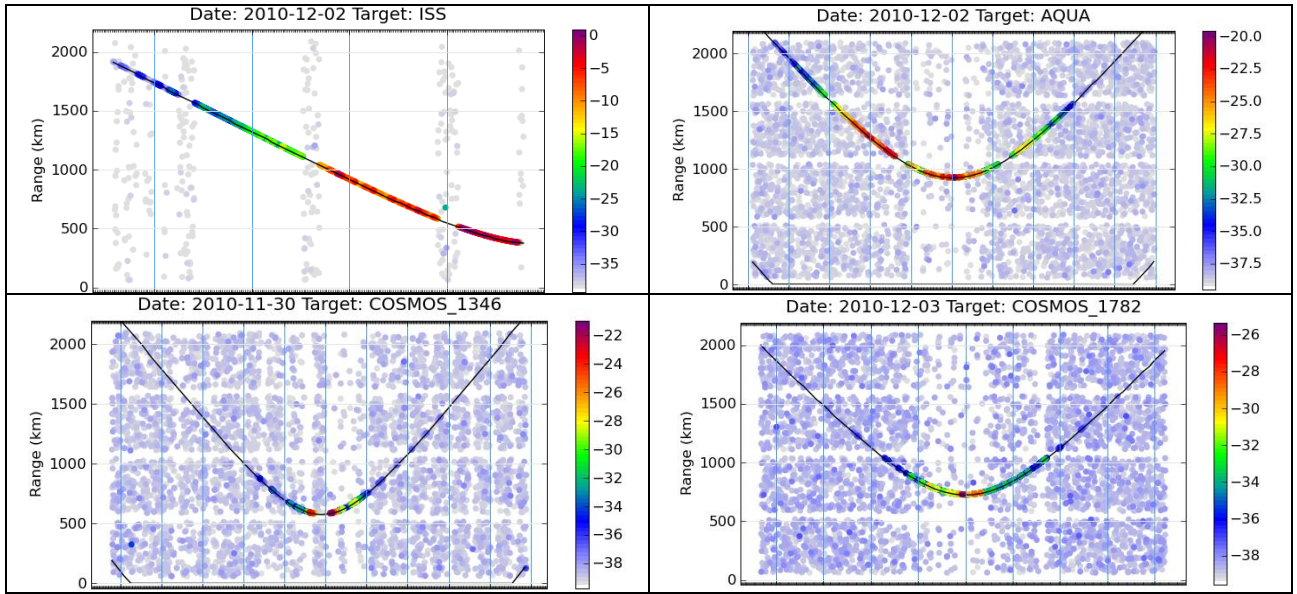


Fig. 6 (a-d). Tracks for a) the ISS, b) AQUA, c) COSMOS_1346 and d) COSMOS_1782: additional targets observed during the initial ESA ‘CO-VI’ tracking campaign

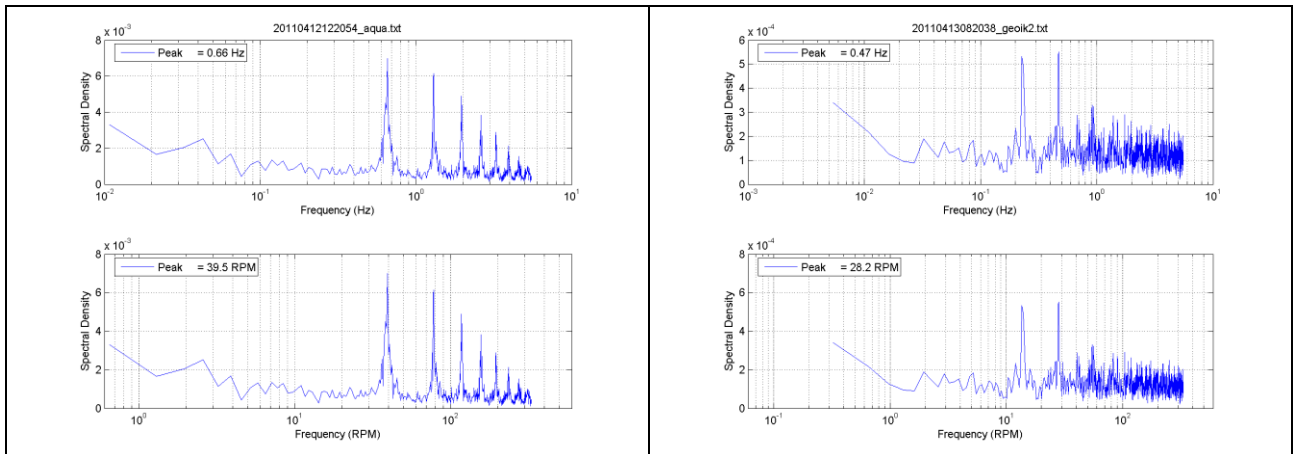


Fig. 7 (a-b). Spectrograms for AQUA and GEO-IK-2 illustrating: (a) detection of a mechanically-scanned instrument on AQUA, and (b) that GEO-IK-2 was tumbling at a rate of 14.1 r.p.m. at the time of observation

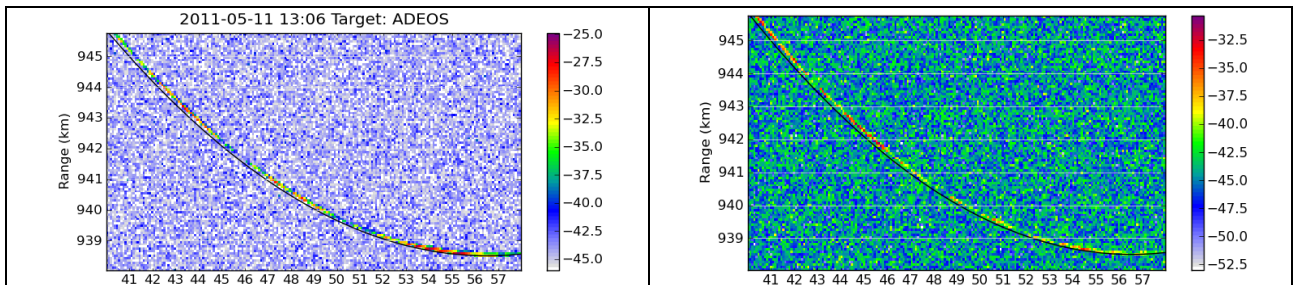


Fig. 8 (a-b). 75 m range-resolution track for ADEOS illustrating that there are times (eg: between seconds 45 and 46) when the co-polar signal level (a) is exceeded by that simultaneously received in the cross-polar channel (b)